

EVALUATION OF THE IMPROVEMENT IN THE FIGURE OF MERIT OF Bi_2Te_3 -BASED ALLOYS WITH ADDITION OF ULTRAFINE SCATTERING CENTERS

Jean-Pierre Fleurial

JetPropulsion Laboratory/ California Institute of Technology,
MS 277-212, 4800 Oak Grove Dr., Pasadena, CA 91109, USA

ABSTRACT

The addition of ultrafine scattering centers into Bi_2Te_3 -based materials and their impact on the thermal and electrical transport properties in a 200-500 K temperature range are discussed. Based on previous theoretical efforts, the resulting improvements in the figure of merit of these heavily doped thermoelectric semiconductors were calculated as a function of composition, temperature, doping level, particulate size and concentration. Determination of the lattice thermal conductivity of the various alloys was conducted by considering phonon-phonon, carrier-phonon, point defect and inert scattering center scattering mechanisms. Degradation of the electrical properties due to the increase scattering rate was also taken into account. Practical application of these results is considered.

INTRODUCTION

Additions of randomly distributed ultrafine particulates into an otherwise undisturbed single crystalline thermoelectric material have been suggested as a possible mechanism to scatter intermediate wavelength phonons and decrease the lattice thermal conductivity. Calculations performed for Si-Ge alloys [1-3] determined that 10 to 40% improvement in the figure of merit Z might be obtained. Experimental work conducted on hot-pressed p-type Si-Ge alloys with additions of Si_3Ni_4 particulates 50 Å in diameter successfully demonstrated the enhanced Bi_2Te_3 scattering rate [4].

Application of a comprehensive model to the thermal and electrical transport properties of both n-type and p-type Bi_2Te_3 -based alloys for their full temperature range of usefulness was applied very recently [5]. Expressions of all the transport properties of thermoelectric semiconductors were derived from the Boltzmann's transport equation, using the relaxation time approximation [6]. This widely used method has been employed with Fermi statistics to calculate carrier mobility, electrical

conductivity, carrier concentration, Hall coefficient, Seebeck coefficient, electronic and bipolar contribution to the thermal conductivity as well as other transport coefficients. Effect of minority carrier conduction and complex band structures were taken into account by the model: up to two conduction bands and two valence bands were considered. The two most common carrier scattering mechanisms usually necessary to describe the transport properties in these heavy doping conditions were selected: acoustic phonon scattering and ionized impurity scattering. Based on the relative changes in thermal conductivity with the composition of the alloys, the model predicted maximum room temperature ZT of $3.5-3.6 \times 10^{-3} K^{-1}$. These values corresponded to about a 40% improvement above commercially available materials and a 10-20% increase above the best results reliably achieved in the laboratory on single crystalline samples.

In continuation of this work, the model was applied to the calculation of the changes in lattice thermal conductivity of Bi_2Te_3 -based alloys by introducing inert scattering centers. Their impact on the thermal and electrical transport properties in a 200-500 K temperature range are discussed. Determination of the lattice thermal conductivity of the various alloys was conducted by considering phonon-phonon, carrier-phonon, point defect and inert scattering center scattering mechanisms. Degradation of the electrical properties due to the inclusions was also taken into account. The resulting improvements in the dimensionless figure of merit ZT of these heavily doped thermoelectric semiconductors were calculated as a function of composition, temperature, doping level and particulate size and concentration.

THEORETICAL APPROACH

Lattice Thermal Conductivity

Calculation of the lattice thermal conductivity was carried out by using the Boltzmann's equation for phonons and adding scattering by ultrafine electrically and thermally insulating inclusions to the three other scattering mechanisms already considered by the model: normal and Umklapp phonon-phonon scattering, point defect scattering and carrier-phonon scattering. The general expression [7] for the lattice thermal conductivity λ_l is (1):

$$\lambda_l = \frac{k_B}{2\pi^2 v} \left(\frac{k_B T}{h} \right)^3 \left[\frac{1}{v_1} + \frac{1}{v_2} + \frac{1}{v_3} \right] \quad (1)$$

$$\text{with } \tau_1 = \int_0^{0.1} \tau_c \frac{x^4 \exp(x)}{[\exp(x) - 1]^2} dx \quad (2)$$

$$\tau_2 = \beta \int_0^{0.1} \frac{\tau_c}{\tau_u} \frac{x^4 \exp(x)}{[\exp(x) - 1]^2} dx \quad (3)$$

$$\tau_3 = \beta \int_0^{0.1} \frac{1}{\tau_u} \left(1 - \beta \frac{\tau_c}{\tau_u} \right) \frac{x^4 \exp(x)}{[\exp(x) - 1]^2} dx \quad (4)$$

where $(\tau_c)^{-1}$ represents the total phonon scattering rate, τ_u is the relaxation time due to three-phonon Umklapp processes, β is the ratio of the Umklapp to normal phonon-phonon relaxation times and x is the reduced phonon frequency $\frac{\hbar\omega}{k_B T}$. The total phonon scattering rate is determined from (5)

$$\frac{1}{\tau_c} = \frac{1}{\tau_u} + \frac{1}{\tau_{pd}} + \frac{1}{\tau_c} + \frac{1}{\tau_{sc}} \quad (5)$$

where τ_{pd} is the relaxation time due to point defect scattering and τ_c is the relaxation time due to carrier-phonon scattering. Expressions for these relaxation times were given earlier [5].

The phonon relaxation time due to ultrafine scattering centers, assuming a spherical inclusion, is [8]:

$$\frac{1}{\tau_{sc}} = N A v \quad (6)$$

where N corresponds to number of inclusions per unit volume and A is the cross-sections area of the inclusions. Rewriting (6) in terms of c , the volume fraction of inclusions, and d , their diameter, an expression (7) very similar to the one derived for grain boundary scattering [3] is obtained:

$$\frac{1}{\tau_{sc}} = \frac{3c}{d} v \quad (7)$$

This expression shows that the smaller the diameter and the larger the volume fraction of inclusions, the higher the scattering rate and thus the lower the lattice thermal conductivity.

Electrical transport properties

Corrections to the bulk transport properties can be estimated, by considering theoretical work done on the transport properties of heterogeneous materials. Expressing the effective electrical conductivity σ as a Fourier series about the volume-averaged

value and considering an isotropic medium in which the variations in electrical conductivity have no preferred direction [9, 10], one obtains the following expression (8):

$$\sigma = \sigma_0 \left[1 - \frac{1}{3} \frac{\langle \Delta \sigma^2 \rangle}{\sigma_0^2} \right] \quad (8)$$

where σ_0 is the volume-averaged value and $\langle \Delta \sigma^2 \rangle$ corresponds to an integrated average of the variations in conductivity. Considering a composite material consisting of a continuous matrix of Bi_2Te_3 -based alloy of electrical conductivity σ_{BiTe} and of ultrafine scattering inclusions of electrical conductivity σ_{sc} , expressions (9) and (10) for σ_0 and $\langle \Delta \sigma^2 \rangle$ can be written as a function of c , σ_{BiTe} and σ_{sc}

$$\sigma_0 = (1 - c) \sigma_{\text{BiTe}} + c \sigma_{\text{sc}} \approx (1 - c) \sigma_{\text{BiTe}} \quad (9)$$

$$\langle \Delta \sigma^2 \rangle = c(1 - c) (\sigma_{\text{BiTe}}^2 - \sigma_{\text{sc}}^2) \approx c(1 - c) \sigma_{\text{BiTe}}^2 \quad (10)$$

Because the inclusions are perfect electrical insulators, the expressions of (9) and (10) were modified considering that $\sigma_{\text{BiTe}} \gg \sigma_{\text{sc}}$. Using (9) and (10), (8) can be rewritten as (11), only function of c and σ_{BiTe}

$$\sigma = \sigma_{\text{BiTe}} \left(1 - \frac{4c}{3} \right) \quad (11)$$

From (11), it is clear that the larger the volume fraction of the inclusions, the larger the decrease in electrical conductivity. Using a similar approach considering perfect thermal insulators, an analogous relationship (12) is obtained for the thermal conductivity:

$$\lambda = \lambda_{\text{BiTe}} \left(1 - \frac{4c}{3} \right) \quad (12)$$

So, in the case of perfect electrical and thermal insulators such as voids, corrections to the electrical and the thermal conductivity cancel each other in the expression of ZT . An identical end result is obtained in the case of perfectly electrically and thermally conducting inclusions, by calculating the perturbations on the electrical and thermal resistivity this time [10]. The total thermal conductivity is determined by adding up the lattice (1), electrical (13) and bipolar (14) contributions in (15):

$$\lambda_e = L \sigma T \quad (13)$$

$$\lambda_{\text{bip}} = \frac{1}{2\sigma} \left[\sum_{i,j} \sigma_i \sigma_j (S_i - S_j)^2 \right] T \quad (14)$$

$$\lambda = \lambda_l + \lambda_e + \lambda_{\text{bip}} \quad (15)$$

where L is the Lorenz number, σ_i and S_i are the individual electrical conductivity and Seebeck coefficient of each valence or conduction band.

In (13) and (14), the electronic contribution to the thermal conductivity, $\lambda_e \approx \lambda_{bip}$, is affected by the same correction to the electrical conductivity as in (11). However, to be consistent with (12), the lattice contribution to the thermal conductivity (λ_l) needs to be multiplied by the same factor in addition to the expected decrease due to an enhanced phonon scattering rate.

To estimate the correction to the Seebeck coefficient, exact calculations [11] relating the effective electrical conductivity σ (at zero temperature gradient), thermal conductivity γ (at zero electric field) and Seebeck coefficient S to the individual contributions of the Bi_2Te_3 -based matrix and scattering inclusion were used (16):

$$\begin{aligned} S - S_{sc} &= \frac{\gamma - \gamma_{sc}}{\sigma - \sigma_{sc}} \\ S_{\text{BiTe}} - S_{sc} &= \frac{\gamma_{\text{BiTe}} - \gamma_{sc}}{\sigma_{\text{BiTe}} - \sigma_{sc}} \end{aligned} \quad (16)$$

Considering that $\sigma_{\text{BiTe}} \gg \sigma_{sc}$ for electrically insulating inclusions, (17) is obtained:

$$\frac{S - S_{sc}}{S_{\text{BiTe}} - S_{sc}} \approx 1 \quad (17)$$

$$\text{or,} \\ S \approx S_{\text{BiTe}} \quad (18)$$

CALCULATED TRANSPORT PROPERTIES

Improved fit to experimental data

The set of adjustable transport parameters (such as effective mass, β ratio, dielectric constant) previously determined to fit quite satisfactorily the retype experimental data on Bi_2Te_3 -based alloys was used [5]. A new set of adjustable parameters was obtained for p-type Bi_2Te_3 -based alloys which resulted in a much better overall fit of all the transport coefficients, including ZT . This was achieved by including ZT in the set of experimental data to be fitted. The experimental data sets to be fitted consisted of a number of data points providing temperature T , composition, electrical conductivity σ , Hall mobility μ_H , Seebeck coefficient S , thermal conductivity λ and dimensionless figure of merit ZT . Determination of the adjustable parameters was achieved by

minimizing the statistical χ^2 function in (9), using a generalized non-linear square fit technique [12]:

$$\chi^2 = \sum_{i=1}^n w_i^o \left(1 - \frac{O_i^{\text{exp}}}{O_i}\right)^2 + \sum_{i=1}^n w_i^u \left(1 - \frac{U_i^{\text{exp}}}{U_i}\right)^2 + \sum_{i=1}^n w_i^s \left(1 - \frac{S_i^{\text{exp}}}{S_i}\right)^2 + \sum_{i=1}^n w_i^\lambda \left(1 - \frac{\lambda_i^{\text{exp}}}{\lambda_i} y\right)^2 + \sum_{i=1}^n w_i^{ZT} \left(1 - \frac{ZT_i^{\text{exp}}}{ZT_i}\right)^2 \quad (19)$$

where the different weighting factors w_i are equal to 1 or 0 depending on whether the corresponding experimental data is or is not known. The total number of degrees of freedom N_{DF} indicates to what extent the fit is over determined; and is calculated as the total number of experimental properties provided plus 1, reduced by the total number of adjustable parameters:

$$N_{\text{DF}} = \sum_{i=1}^n w_i^o + \sum_{i=1}^n w_i^u + \sum_{i=1}^n w_i^s + \sum_{i=1}^n w_i^\lambda + \sum_{i=1}^n w_i^{ZT} + 1 - (n_{\text{adj}} + n) \quad (20)$$

This approach was justified by the fact that Z is a complex combination of the other transport properties. No guidelines were built into the model to insure that the values of Z were consistent with those calculated from experimental data, even if a good fit was achieved on the electrical resistivity, the Seebeck coefficient and the thermal conductivity. As a result, a single least-squares fit simultaneously applied to all of the selected p-type experimental data resulted in a root-mean-square deviation between the calculated and observed values of about $\pm 1\%$, a very remarkable agreement. This good agreement between calculated and "experimental" ZT values is shown on Figure 1.

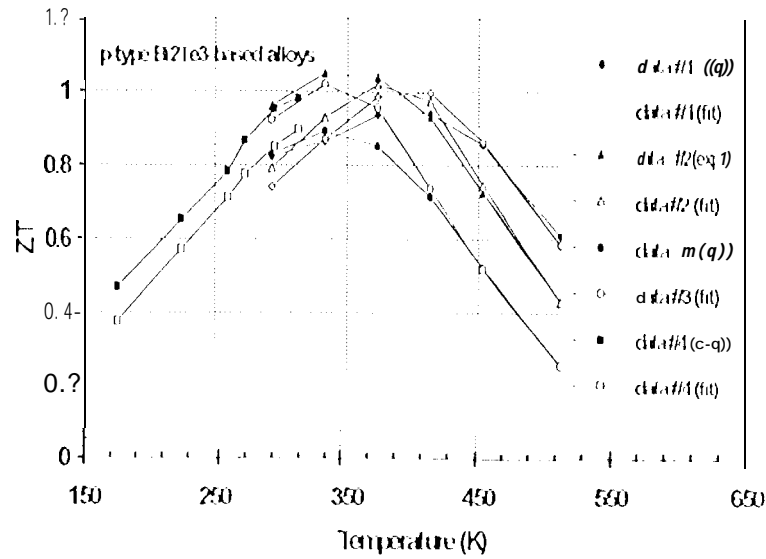


Fig. 1 Improved fit to ZT values calculated from experimental Seebeck coefficient, electrical resistivity and thermal conductivity data.

Notice that the maximum Z values are now well reproduced by the model. Figures 2 and 3 display calculated ZT values as a function of carrier concentration, for various temperatures (Figure 2) and various compositions (Figure 3). As predicted earlier [5], the maximum ZT values at 300 K are close to 1.05.

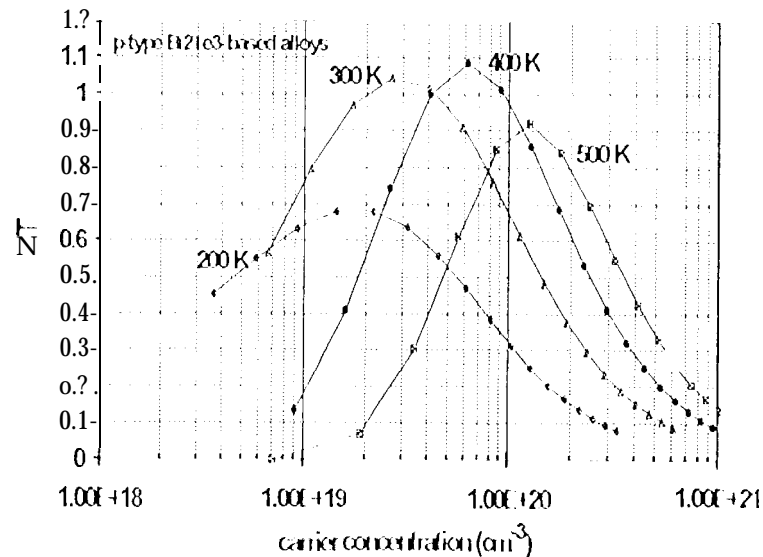


Fig. 2 Extrapolated ZT values at 200, 300, 400, and 500 K as a function of carrier concentration for $(\text{Bi}_2\text{Te}_3)_{0.7}(\text{Sb}_2\text{Te}_3)_{0.7}(\text{Bi}_2\text{Se}_3)_{0.1}$ p-type alloy.

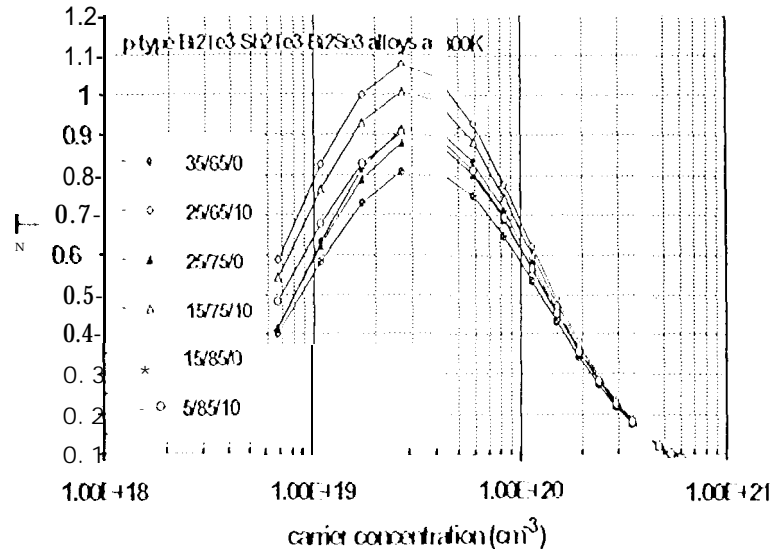


Fig. 3 Extrapolated ZT values at 300K as a function of carrier concentration for several Sb_2Te_3 -rich $(\text{Sb}_2\text{Te}_3)_{1-x-y}(\text{Bi}_2\text{Te}_3)_x(\text{Bi}_2\text{Se}_3)_y$ -type alloys.

Using these two sets of adjustable parameters, the model calculated the new transport properties values for a broad range of compositions, carrier concentrations and temperatures, with addition of various volume fractions of spherical ultrafine scattering centers of different diameters.

Addition of ultrafine scattering centers

Because of the tremendous amount of data generated by the model calculations, the results presented in this paper are restricted to representative alloy compositions, temperatures, volume fraction and diameter of inclusions. Also, calculations performed for both n-type and p-type Bi_2Te_3 -based alloys showed very little differences in the magnitude of the changes brought by the addition of the ultrafine scattering centers. Therefore, only one graph (Figure 9) illustrates the results for p-type alloys.

Figure 4 describes the decrease at room temperature of the lattice thermal conductivity of n-type Bi_2Te_3 -based alloys with 6 volume % addition of inclusions of decreasing diameters. Because the carrier-phonon scattering was found to have very little impact on the lattice thermal conductivity [5], results are shown for a constant carrier concentration of about $1.5 \times 10^{19} \text{ cm}^{-3}$. About a 15% reduction in lattice thermal conductivity is obtained by adding 6 volume % of inclusions 20 Å in diameter.

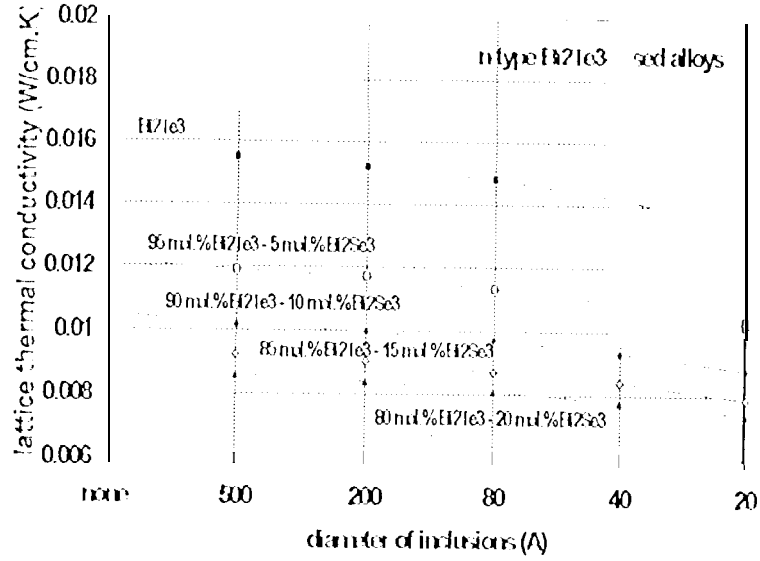


Fig. 4 Lattice thermal conductivity reduction as a function of inclusion diameter (6 volume %) for n-type Bi₂Te₃-based alloys at 300K (carrier concentration $\approx 1.5 \times 10^{19} \text{ cm}^{-3}$).

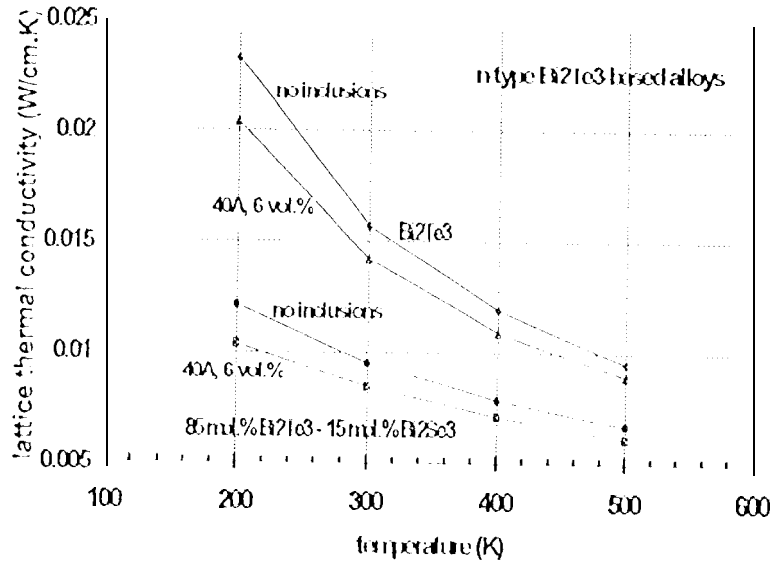


Fig. 5 Lattice thermal conductivity with and without 6 volume % of 40Å diameter inclusions versus temperature for Bi₂Te₃ and (Bi₂Te₃)_{0.85}-(Bi₂Se₃)_{0.15} n-type alloy (carrier concentration $\approx 1.5 \times 10^{19} \text{ cm}^{-3}$).

Figure 5 shows the lattice thermal conductivity as a function of temperature for both n-type Bi₂Te₃ and (Bi₂Te₃)_{0.85}-(Bi₂Se₃)_{0.15} compositions. For each composition, there are two sets of data, one corresponding to the material being free of

inclusions and one to the material with 6 volume % of inclusions 40\AA in diameter. Results are shown for a constant carrier concentration of about $1.5 \times 10^{19} \text{ cm}^{-3}$. These particular values for the size and amount of inclusions were selected because preparing such a material appears feasible (as is done on $\text{Si}_{80}\text{Ge}_{20}$ material [13]) and also because 6 volume % is well within the range covered by the calculated perturbations to the electrical properties. Additions in excess of 10 volume % are very likely to degrade the properties faster than the rate estimated in the previous paragraphs. Figure 5 demonstrates that the relative drop in lattice thermal conductivity due to the ultrafine scattering centers decreases rapidly as temperature increases. This result was expected as the λ_l approximately follows a T^{-1} variation and the traditional phonon scattering mechanisms become more effective.

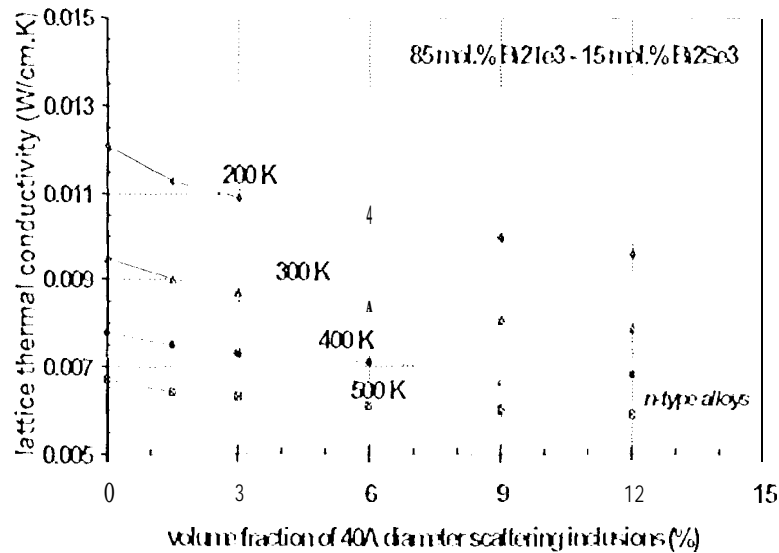


Fig. 6 Reduction in lattice thermal conductivity as a function of the volume fraction of 40\AA diameter inclusions for n-type $(\text{Bi}_2\text{Te}_3)_{0.85}-(\text{Bi}_2\text{Se}_3)_{0.15}$ alloy at temperatures of 200, 300, 400 and 500K (carrier concentration $\approx 1.5 \times 10^{19} \text{ cm}^{-3}$)

The decrease of the lattice thermal conductivity with an increasing volume fraction of 40\AA diameter inclusions is shown on Figure 6 for the same n-type $(\text{Bi}_2\text{Te}_3)_{0.85}-(\text{Bi}_2\text{Se}_3)_{0.15}$ alloy composition. Results are shown at a constant carrier concentration of about $1.5 \times 10^{19} \text{ cm}^{-3}$, for temperatures 200, 300, 400 and 500K. Because the overall corrections to the electrical resistivity and thermal conductivity (equations (11) and (12) for inhomogeneous materials), the reduction in lattice thermal conductivity directly translates into an improvement in ZT. To better visualize this improvement, the relative increase in

maximum ZT has been plotted at temperatures of 200, 300, 400 and 500K as a function of the volume fraction of 40Å diameter inclusions. Figures 7 and 8 show calculation results for an n-type $(\text{Bi}_2\text{Te}_3)_{0.85}-(\text{Bi}_2\text{Se}_3)_{0.15}$ alloy and a p-type $(\text{Bi}_2\text{Te}_3)_{0.2}-(\text{Sb}_2\text{Te}_3)_{0.7}-(\text{Bi}_2\text{Se}_3)_{0.1}$ alloy, respectively. The improvement in maximum ZT (at optimum doping level) is very similar in both n-type and p-type sample, due to the weakness of both the phonon-electron and the phonon-hole scattering rates.

Figures 7 and 8 convincingly show that a practical maximum improvement of 15-20% can be obtained at the lowest temperatures. However, the benefits of adding ultrafine scattering centers disappear quickly with increasing temperature as the phonon-phonon scattering rates increase rapidly (T^{-1} variation of the lattice thermal conductivity). At the highest temperature of use for Bi_2Te_3 -based alloys, the relative improvement in maximum ZT is under 5%.

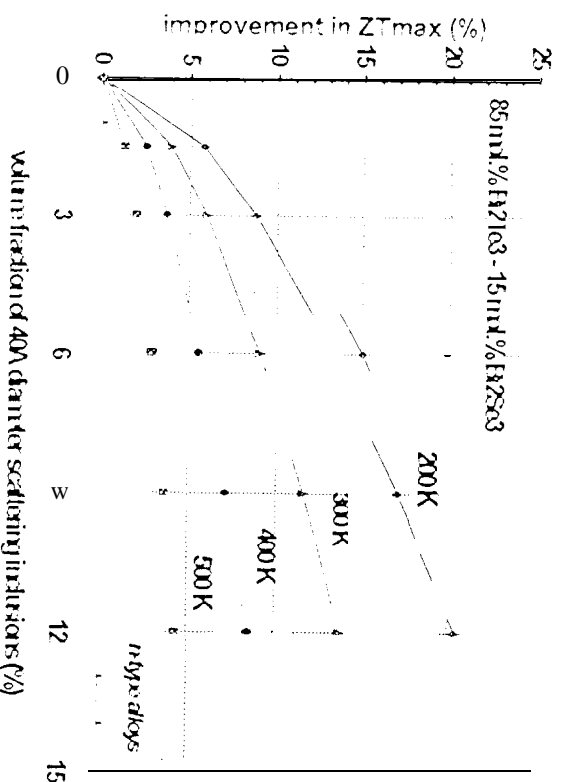


Fig. 7 Relative improvement in maximum ZT with increasing volume fraction of inclusions 40Å in diameter for $(\text{Bi}_2\text{Te}_3)_{0.85}-(\text{Bi}_2\text{Se}_3)_{0.15}$ n-type alloy at 200, 300, 400 and 500K.

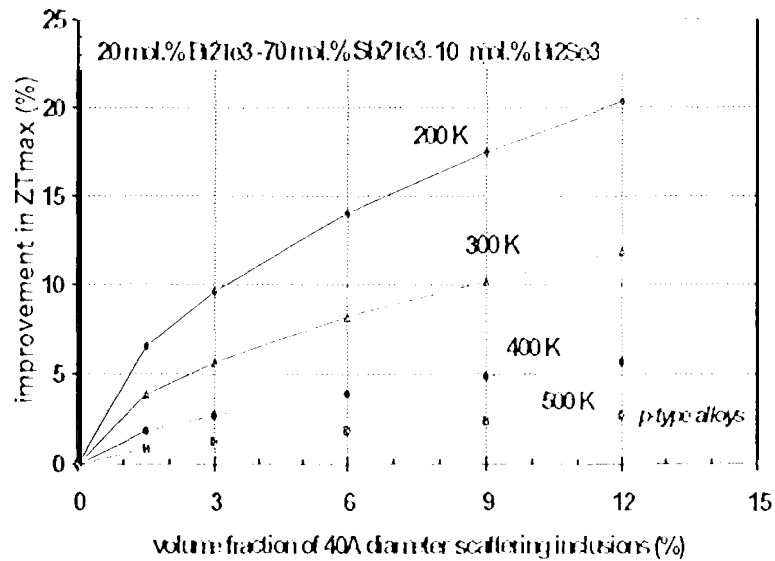


Fig. 8 Relative improvement in maximum ZT with increasing volume fraction of inclusions 40Å in diameter for $(\text{Bi}_2\text{Te}_3)_{0.2}\text{-(Sb}_2\text{Te}_3)_{0.7}\text{-(Bi}_2\text{Se}_3)_{0.1}$ p-type alloy at 200, 300, 400 and 500K.

Even if a 20% improvement in ZT at 200K constitutes a significant increase, one should not forget that achieving such a result in practice on Bi_2Te_3 -based alloys could be quite difficult. From a theoretical point of view, additional scattering mechanisms need to be taken into account as ZT cannot increase indefinitely with an increasing volume fraction of inclusions. A minimum lattice thermal conductivity cutoff must be introduced in equation (5) as the phonon mean free path cannot be reduced too low. Also, though no overall degradation in τ_c^{-1} (not accounting for phonon scattering mechanisms which lower λ_1 and thus improve ZT) is obtained for small additions of perfectly conducting or insulating inclusions (both thermally and electrically), larger additions cannot be treated theoretically as a perturbation and other approximations are required (percolation theory). From a practical point of view, the preparation of good quality Bi_2Te_3 -based alloys with 6 to 10 volume % of 40Å diameter inclusions is a real challenge. Such experimental work is in progress on hot-pressed SiGe thermoelectric alloys [13]. Some difficult problems have been solved and some encouraging results have been obtained, but the nature and the reproducibility of the improvements are hard to control. Often it is difficult to distinguish between effects due to grain size, dopant concentration or sample quality from genuine inert inclusions scattering effects. High quality single crystalline or large grain polycrystalline Bi_2Te_3 -based materials are prepared by directional

solidification from a melt. These alloys have anisotropic properties, and highest Z values are obtained parallel to the growth direction [14]. To prepare Bi_2Te_3 -based samples with additions of randomly distributed ultrafine inclusions, the use of powder metallurgy techniques is required. As a consequence, it is highly probable that any improvement in lattice thermal conductivity will be negated by the losses in electrical transport properties due to small and/or disoriented grains.

CONCLUSION

Building on the transport properties model previously developed for n -type and p -type Bi_2Te_3 -based alloys, corrections and modifications were made to both improve the fit to the existing experimental database and to account for the effect of the inclusions on all transport coefficients. By imposing ZT as an "experimental" transport property to the generalized fitting routines, a much better overall agreement between calculated and experimental values was achieved, the model maximum ZT values of 1.05-1.1 at 300K.

Detailed analysis of the variations in bulk properties (theory of inhomogeneous alloys) and phonon scattering rates (theory of lattice thermal conductivity) showed that in the case of perfect electrical and thermal insulators, the changes in ZT depend only on the decrease in lattice thermal conductivity. Calculations done with 6 to 10 volume fraction of 40 Å diameter inclusions predicted that about 15 to 20% improvement in maximum ZT is possible at low temperatures (200 to 300K) but that much smaller increases, 5 to 10%, are likely at high temperatures (400 to 500K). Although 15 to 20% improvement is not negligible for a state-of-the-art material, practical considerations on the preparation and quality of such samples with additions of ultrafine inclusions drastically reduce its attractiveness.

ACKNOWLEDGMENTS

The work described in this paper was carried out by the Jet Propulsion Laboratory/California Institute of Technology, under a contract with the National Aeronautics and Space Administration. This effort was sponsored by the Knolls Atomic Power Laboratory, Schenectady, New York. The author would like to thank Dr. Paul Klemens and Dr. Cronin Vining for many helpful discussions.

REFERENCES

- [1] P.G. Klemens, "Thermal Conductivity of n -type Si-Ge", in *Modern Perspectives on Thermoelectrics and Related*

- Materials*, MRS Symp. 11th oc. Vol. 234, 87-94, (Materials Research Society, Pittsburg, Pennsylvania 1991).
- [2] C.B. Vining, "A Model for the High Temperature Transport Properties of Heavily Doped p-type Silicon-Germanium Alloys", in *Modern Perspectives on Thermoelectrics and Related Materials*, MRS Symp. Proc. Vol. 234, 95-104, (Materials Research Society, Pittsburg, Pennsylvania 1991).
 - [3] G. A. Slack and M.A. Hussain, "The maximum possible conversion efficiency of silicon-germanium thermoelectric generators", *J. appl. Phys.*, 70 (5), 2694 (1991)
 - [4] J.S. Beaty, J.L. Rolfe and J. W. Vandersande, "Thermoelectric Properties of Hot-Pressed Ultrafine Particulate SiGe Powder Alloys with Inert Additions", in *Modern Perspectives on Thermoelectrics and Related Materials*, MRS Symp. Proc. Vol 234, 105-109, (Materials Research Society, Pittsburg, Pennsylvania 1991)
 - [5] J.-P. Fleurial, "Thermal and Electrical Transport Properties Modeling Of Bi₂Te₃-based alloys", *Proceedings of the XIth International Conference on Thermoelectrics*, Arlington, Texas, USA, October 7-9, p. 276-281 (1997)
 - [6] V.J. Fistul, "Heavily Doped Semiconductors", Plenum, New York (1969).
 - [7] J. Callaway, H.C. von Bayer, *Phys. Rev.*, 120, 1149 (1960)
 - [8] D.P. White and P.G. Klemens, "Thermal conductivity of thermoelectric Si_{0.8}-Ge_{0.2} alloys", *J. Appl Phys.*, 71 (9), 4258 (1997).
 - [9] P.G. Klemens "Thermal Conductivity of Inhomogeneous Materials" in *Thermal Conductivity 21*, Edited by C. L. Cremers and H.A. Fine, Plenum Press, New York, 383-390 (1991)
 - [10] P.G. Klemens, "Electrical resistivity Of inhomogeneous alloys", *J. Appl. Phys.*, 70 (8), 4322 (1991)
 - [11] D.J. Bergman and O. Levy, "Composite Thermoelectrics- Exact Results and Computational Methods", in *Modern Perspectives on Thermoelectrics and Related Materials*, MRS Symp. Proc. Vol. 234, 39-45, (Materials Research Society, Pittsburg, Pennsylvania 1991).
 - [12] Numerical Recipes in C, [w.] J. Press and al., Cambridge University, Cambridge, UK (1985)

- [13] J.W. Vandersande, J.-P. Fleurial, J.S. Beaty and J.J. Rofe
 "Addition of Fine Scattering Centers for Thermal
 Conductivity Reduction in p-type $\text{Si}_{80}\text{Ge}_{20}$ ", *Proceedings of
 the XIth International Conference on Thermoelectrics*,
 Arlington, Texas, USA, October 7-9, p. 21-23 (1992),
- [14] S. Scherrer, H. Scherrer and T. Caillat, "Recent
 Developments in Compounds Tellurides and their Alloys for
 Peltier Cooling", *Proceedings of the IXth International
 Conference on Thermoelectrics*, Pasadena, California,
 March 19-21, (1), 1-15(1990).